Iran University of Science and Technology

International Journal of

Railway Research

ISSN: 2423-3838

An Efficient Modal Parameter Identification Method Based on Free Vibration Response and the Energy Sorted Matrix Pencil Method

Mohammad Sadegh Ayubirad[1], Shervan Ataei[1*]

[1]School of Railway Engineering, Iran University of Science and Technology, Tehran

ARTICLE INFO

Article history:
Received: 10.03.2024
Accepted: 08.06.2024
Published: 10.06.2024

Keywords:
Damping ratio
Frequency estimation
Railway bridges
Structural health monitoring
Train loading

A B S T R A C T

Modal parameter identification of railway bridges is essential for comprehending their dynamic behavior. This understanding enables the development of numerical simulations that more accurately mirror their actual behavior. It also helps in monitoring changes in material condition through frequency variations over time and establishing the maximum speeds for trains crossing the bridge, all of which contribute to more effective and efficient management of infrastructure. This research presents a feasible and efficient methodology for determining the modal characteristics of railway bridges through analyzing their free vibration response. The methodology employs the energy sorted matrix pencil method (MPM). The standard MPM is known to identify both dominant and trivial modes, which can lead to erroneous results. By differentiating modes based on their energy levels, it is possible to isolate the dominant modes effectively, thereby avoiding the issues of mode mixing and mode splitting. Following an initial verification using synthetic multi-modal signals, the energy-sorted MPM is implemented in a real-world case study. It focuses on the modal parameter identification of a truss railway bridge under impact and service loads. The modal frequency and damping ratios were determined by analyzing the free decay responses. These identified modal damping ratios, observed under operational loads, were analyzed in comparison to those detected under impact tests. The successful application of the energy sorted MPM method in both theoretical and practical frameworks highlights its potential for structural health monitoring and maintenance of critical railway infrastructure.

1. Introduction

Railway bridges are a critical component of rail transportation networks. The current state of railway bridge infrastructure, however, is deteriorating quickly. Many railway bridges have reached or are nearing the expiration of their intended lifespan. The growing need for faster trains, heavier loads, and longer train compositions calls for an improved evaluation of the dynamic performance of railway bridges to ensure their safety [1–3]. Modal parameter identification serves as a reliable nondestructive approach for evaluating the current state of a structure. The modal characteristics derived from the dynamic response of a structure closely correspond to its fundamental physical attributes, including mass, stiffness, and the ability to dissipate energy. These characteristics offer a practical means for overseeing the overall behavior of the structure. Moreover, changes in these characteristics over time can be instrumental in identifying and monitoring structural damage. Consequently, accurately determining modal frequencies, damping ratios,

*Corresponding author
Email address: ataei@iust.ac.ir

[DOI: 10.22068/ijrare.349]

and mode shapes is vital for finite element (FE) model updating of structural systems [4,5]. Free vibration tests emerge as a practical solution for experimental dynamic characterization. These tests, which can be conducted once, periodically, or after specific events, rely on temporarily installed sparse sensor networks. Such setups are characterized by their limited cost, reduced technical complexity, and minimal environmental interference, making them particularly suited for rapid information gathering on the dynamic behavior of railway bridges. Free vibration tests offer the benefit of generating responses at higher excitation levels than ambient vibrations, which improves the signal-to-noise ratio (SNR) and reduces noise influence [6].

In this context, Yang et al. [7] employed a free vibration response detection algorithm on high-speed railway bridges to aid in modal identification. They utilized the iterative variational mode decomposition (IVMD) method to adaptively extract modal components from vibration data and employed the eigensystem realization algorithm (ERA) for modal parameter identification. Mazzeo et al. [4,6] used the variational mode decomposition (VMD) and the empirical Fourier decomposition (EFD) techniques for automatic modal identification of highway bridges based on free vibration response. The results from comparing the VMD and EFD techniques showed that the EFD-based methodology provides more consistent estimates of modal parameters.

However, these methods still rely on traditional damping identification techniques, such as the logarithmic decrement (LD) method, curve fitting [8–10], and the area ratio-based method [11], which were primarily developed for single-degree-of-freedom (SDOF) systems. To apply these techniques to MDOF systems, the modal components must first be accurately extracted using the aforementioned decomposition methods. This process can be challenging, as it may lead to mode-mixing or mode-splitting issues, particularly when the natural frequencies of the system are closely spaced. Inaccuracies in the modal component extraction can propagate through the damping identification process, leading to erroneous results. Therefore, while VMD and EFD techniques have advanced modal identification in MDOF systems, there remains a need for a more direct and reliable approach to damping identification that can circumvent the potential pitfalls associated with modal component extraction.

To address the limitations of existing damping identification methods in MDOF systems, the energy-sorted matrix pencil method (MPM) has been proposed as a more direct and reliable approach [12]. The main advantage of the MPM lies in its ability to identify modal parameters, including damping ratios, directly from the free vibration response of an MDOF system without the need for prior extraction of individual modal components.

Recently, Silva et al. [13] used the energy-sorting Prony method to evaluate damping coefficients in railway bridges by analyzing dominant frequencies in vibrations caused by trains, contributing to updates in the filler-beam railway bridge damping coefficient database for future EN1991-2 revisions. However, the MPM outperforms the Prony technique in identifying modes from noisy signals because it utilizes the singular value decomposition (SVD) of the data matrix. SVD allows for a non-iterative way to establish a reduced model order. It also serves as a method for filtering out noise [14].

The authors note a lack of applications and comparative studies on estimating modal parameters in real structures with the MPM. This shortage hinders the comprehension of its precision and dependability in dynamic identification. The present study aims to fill the gap identified in existing research.

This paper presents a computational framework designed for determining the modal properties of railway bridges using their free vibration response. The technique described here employs the MPM as its core. The framework is first tested using synthetic multi-modal signals. Next, the paper presents a practical example, emphasizing the detailed modal identification of a truss railway bridge. The results highlight the effectiveness of this computational framework as a powerful tool for deducing the modal properties of railway bridges by leveraging their free vibration response.

2. Modal identification based on the energy-sorted MPM

This section outlines the entire process of the energy-sorted MPM for identifying the modal

[DOI: 10.22068/ijrare.349]

properties of railway bridges using only their free vibration response. While the method is versatile and applicable to various structures, this research focuses exclusively on analyzing the dynamic behavior of railway bridges. The approach utilizes an appropriate decomposition method to isolate modal components, enabling the estimation of modal frequencies, damping ratios, and mode shapes.

2.1. The MPM

In 1795, Gaspard de Prony [15] introduced a technique for modeling gas expansion as a combination of decaying complex exponential signals based on evenly spaced observations. This method, known as Prony's method, represents a sequence of data points as a sum of complex exponentials characterized by unique amplitudes, damping rates, frequencies, and phases. Its primary innovation lies in simplifying the complex task of exponential approximation into solving linear equations and a root-finding challenge. The method involves creating an autoregressive model to predict each data point from its predecessors, leading to a characteristic polynomial whose roots determine the damping and frequency parameters. These roots then help in calculating the amplitude and phase for each exponential function.

Originally designed to fit a dataset exactly with twice as many points as exponential terms, Prony's method adapts to larger datasets through least squares approximation, typically assuming noise only affects the observed data. Despite its utility, Prony's method can suffer from numerical instability, particularly when dealing with a large number of exponential terms, due to the sensitivity of the polynomial's roots to small changes in their coefficients [16].

Another option is to employ the MPM. While it bears resemblance to Prony's method, it involves addressing an eigenvalue problem instead of the traditional two-step approach associated with Prony's method. Perturbation analysis and simulations have demonstrated that the MPM exhibits lower sensitivity to noise compared to the polynomial method for signals whose damping factors are not known [17]. The sum of L complex parameters can represent a data sequence $z[n]$ for n = 1, ..., N, as per the expression given:

$$z[n] = \sum_{k=1}^{L} A_k\, e^{j\theta_k} \cdot e^{(\alpha_k + j2\pi f_k)T_s(n-1)} = \sum_{k=1}^{L} R_k \cdot \lambda_k^{(n-1)} \quad (1)$$

The signal $z[n]$ is approximated using L components, where A_k represents the starting amplitude in the same units as $z[n]$, α_k denotes the damping factor in per seconds, f_k indicates the frequency in Hz, T_s refers to the sampling period (in seconds), and θ_k is the initial phase in radians. Consequently, the characteristics of signal $z[n]$ are defined by the parameters A_k, α_k, f_k, and θ_k (k = 1, …, L). R_k stands for the time-independent component, and λ_k is the component that is both exponential and dependent on time (poles). In accordance with the MPM methodology, the Hankel matrix, referred to as $\mathbf{Y} \in \mathbb{R}^{(N-L)\times(L+1)}$, is subsequently constructed from the signal data [18]:

$$\mathbf{Y} = \begin{bmatrix} z_0 & z_1 & \cdots & z_L \\ z_1 & z_2 & \cdots & z_{L+1} \\ \vdots & \vdots & \ddots & \vdots \\ z_{N-L-1} & z_{N-L} & \cdots & z_{N-1} \end{bmatrix} \quad (2)$$

where z_n represents the samples, and N signifies the overall count of samples. Also, the pencil parameter, denoted as L, a crucial parameter for eliminating noise from noise-contaminated data, is selected as $N/2-1$ [8]. Following this, the procedure involves computing the SVD of $\mathbf{Y}$ as follows:

$$\mathbf{Y} = \mathbf{U}\mathbf{\Sigma}\mathbf{V}^H \quad (3)$$

where $(\cdot)^H$ represents the complex conjugate transpose, $\mathbf{U}$ and $\mathbf{V}$ denote left and right unitary matrices, respectively, and the diagonal entries of $\mathbf{\Sigma}$ are equal to the singular values (σ_n) of the Hankel matrix, which are then normalized and used to estimate the model order (M) by identifying the number of dominant singular values based on a predefined tolerance threshold (P):

$$\sigma_d \geq 10^{-P}\sigma_{max} \quad (4)$$

where σ_d is the dominant singular value, and σ_{max} is the maximum singular value. For instance, when the data maintains precision to $P = 3$ significant digits, the singular values that fall below the ratio in (4) are fundamentally noise singular values. Consequently, these should not be employed in the data reconstruction process. Hence, the matrix $\mathbf{\Sigma}$ is transformed into $\mathbf{\Sigma}'$ by eliminating the columns

[DOI: 10.22068/ijrare.349]

of singular values that are linked to noise. Subsequently, the $\mathbf{\Sigma}'$ matrix, which includes the dominant singular values, is utilized for the reconstruction of data without noise.

The matrix $\mathbf{V}$ is then transformed into $\mathbf{V}'$ by retaining its columns that are associated with the dominant singular values and discarding the others. Subsequently, two matrices $\mathbf{V}_1'$ and $\mathbf{V}_2'$ are constructed from $\mathbf{V}'$ by respectively removing the last column and the first column of the $\mathbf{V}'$ matrix. The matrices $\mathbf{Y_1}$ and $\mathbf{Y_2}$ are then defined through the following equations [19]:

$$[\mathbf{Y_1}] = [\mathbf{V}_1']^{\boldsymbol{T}}\mathbf{V}_1' \tag{5}$$

$$[\mathbf{Y_2}] = [\mathbf{V}_2']^{\boldsymbol{T}}\mathbf{V}_1' \tag{6}$$

The poles of the system ($\boldsymbol{\lambda} = \mathrm{eig}(\mathrm{pinv}(\mathbf{Y_1}) * \mathbf{Y_2})$), which are derived from the eigenvalues of the matrices $\{[\mathbf{Y_1}], [\mathbf{Y_2}]\}$, enable us to determine the damping and frequency for each mode [17]. Here, $\mathrm{pinv}(\mathbf{Y_1})$ denotes the Moore-Penrose pseudoinverse of the matrix $\mathbf{Y_1}$. The α_k and f_k values are obtained as follows:

$$\alpha_k = \frac{\ln|\lambda_k|}{T_s} \tag{7}$$

$$f_k = \frac{tan^{-1}\left[\frac{Im(\lambda_k)}{Re(\lambda_k)}\right]}{2\pi T_s} \tag{8}$$

2.2. Identifying the dominant frequencies via the energy sorting technique

Upon determining M and the λ_k, the residues, denoted as $\mathbf{R}$, are computed from the subsequent least-squares problem [18]:

$$\begin{bmatrix} z_0 \\ z_1 \\ \vdots \\ z_{N-1} \end{bmatrix} = \begin{bmatrix} 1 & 1 & \cdots & 1 \\ \lambda_1 & \lambda_2 & \cdots & \lambda_M \\ \lambda_1^2 & \lambda_2^2 & \cdots & \lambda_M^2 \\ \vdots & \vdots & \ddots & \vdots \\ \lambda_1^{N-1} & \lambda_2^{N-1} & \cdots & \lambda_M^{N-1} \end{bmatrix} \begin{bmatrix} R_1 \\ R_2 \\ \vdots \\ R_M \end{bmatrix} \tag{9}$$

Here, $\mathbf{R}$ is the vector containing the complex amplitudes associated with each eigenvalue, and the operation aims to find the best fit of the model to the data. The R_k values yield the A_k and θ_k as follows:

$$A_k = |R_k| \tag{10}$$

$$\theta_k = \tan^{-1}\left[\frac{Im(R_k)}{Re(R_k)}\right] \tag{11}$$

Finally, in order to determine the significance of each mode, the energy content, E_i, is calculated for each eigenvalue. Once these energy values are computed, the modes are sorted in descending order based on their energy content. The mode with the highest energy content is placed at the forefront, indicating its dominance within the system. The energy of each mode can be calculated based on the magnitude of the residues (R) and the eigenvalues (λ_i). The energy E_i of the i[th] mode over N samples can be represented as:

$$E_i = \sum_{j=0}^{N-1}\left(\Re\left(\mathbf{R}[i]\cdot\lambda_i^j\right)\right)^2 \tag{12}$$

where $\Re(\cdot)$ denotes the real part of a complex number.

2.3. Identifying the mode shapes

Mode shape identification relies on the analysis of free vibration responses from sensors [4,6,20]. The time point t_p^{peak} corresponds to a local peak (either maximum or minimum) in the k^{th} modal response, found by decomposing the vibration response. The local peak value $v_k^{(s)}\left(t_p^{\text{peak}}\right)$ for the k^{th} modal response from the s^{th} sensor (with S total sensors) is used to calculate the normalized mode shape vector:

$$\overline{\phi}_k = \left\{v_k^{(1)}\left(t_p^{\text{peak}}\right) \quad \ldots v_k^{(s)}\left(t_p^{\text{peak}}\right) \quad \ldots v_k^{(S)}\left(t_p^{\text{peak}}\right)\right\}^T / \max_{1\le s\le S}\left|v_k^{(s)}\left(t_p^{\max}\right)\right| \tag{13}$$

To reduce inaccuracies in identifying modal shapes caused by measurement noise, the normalized mode shape vector is reassessed at each local peak, and each element is estimated by averaging these recalculated values.

3. Numerical validation

3.1. Generation of synthetic signals

The energy-sorted MPM has been rigorously tested using synthetic signals to accurately and objectively evaluate its precision and stability. To achieve this, the response to free vibration of a civil structure with multiple degrees of freedom (MDOF) is typically represented by:

$$f(t) = \sum_{n=1}^{N} A_n\, e^{-\xi_n\omega_n t}\, cos(\,\overline{\omega}_n t - \varphi_n) + w(t) \tag{14}$$

where A_n, ξ_n, ω_n, $\overline{\omega}_n$, φ_n, and $w(t)$ represent the amplitude, modal damping ratio, modal circular frequency, circular damped frequency, phase, and measurement noise, respectively. Data devoid of noise are utilized to assess accuracy in reference conditions. In

[DOI: 10.22068/ijrare.349]

contrast, data with noise are examined to determine and evaluate the identification's resilience under conditions that mimic real-world monitoring more closely. The measurement noise is produced as white Gaussian noise characterized by a specific signal-to-noise ratio (SNR):

$$SNR = 10 \log_{10} \left(\frac{P_s}{P_n}\right) \quad (15)$$

where P_s and P_n represent the average power of the signal and noise, respectively. As the SNR decreases, the presence of noise in the signal intensifies. The simulation covers three specific noise intensities: 0 dB, 5 dB, and 15 dB (it is highlighted that the generated synthetic noisy signals do not undergo initial denoising). Due to the intrinsic variability of the noise, for each level of noise, a collection of 100 independent noisy signals is generated to facilitate a statistical evaluation of the outcomes.

3.2. Synthetic signal with closely spaced modes

A system is characterized by the presence of four modes of vibration, denoted as N=4, in accordance with (14). The amplitudes are A_1=3, A_2=1.8, A_3=1.6, and A_4=5. The modal damping ratios are ξ_1=3%, ξ_2=1.2%, ξ_3=0.8%, and ξ_4 =2%. The natural frequencies are: f_1=1.5 Hz, f_2=3.2 Hz, f_3=3.6 Hz, and f_4=10 Hz. The 2nd and 3rd frequencies are close (i.e., about 10%), which is not common but can occur in civil structures. Moreover, φ_n=0 $\forall n$, and the sampling frequency is F_s=1000 Hz.

Initially, the scenario involving a signal free from noise is examined, leading to the initial condition where the measurement noise is considered to be zero. Figure 1 illustrates the signal in question along with its associated frequency spectrum.

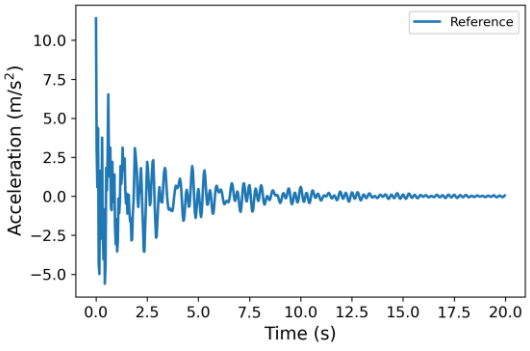

(a)

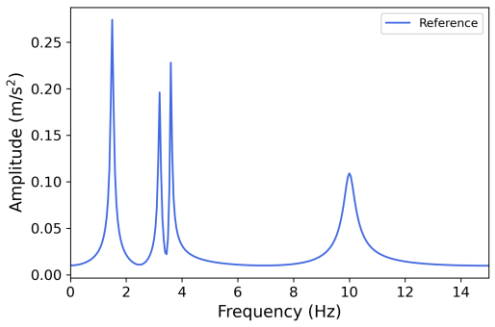

(b)

Figure 1. (a) Noise-free synthetic signal, and (b) frequency spectrum.

Figure 2 illustrates a perfect alignment between the components extracted automatically from the analyzed noise-free synthetic signal and their respective reference analytical modes.

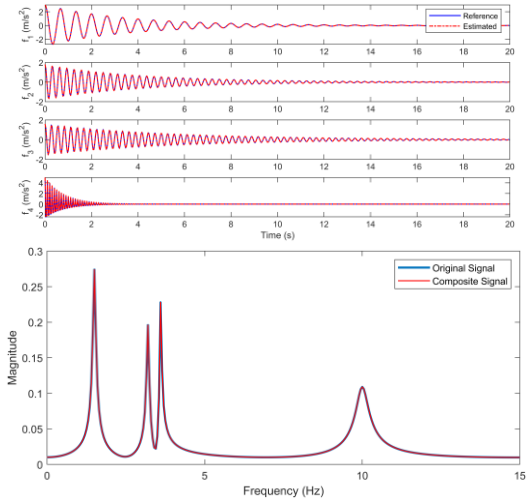

Figure 2. Comparative analysis of the reference analytical modes versus components derived from noise-free data through the energy-sorted MPM.

Table 1 shows the decomposition process of the signal using the energy-sorted MPM. The magnitudes of the identified frequencies, damping ratios, and amplitudes align well with the true analytical values, demonstrating the precision of the method.

Table 1. Decomposition of the multi-component sinusoidal signal using the MPM.

Component	Energy	f [Hz]	ξ [%]	Amplitude
0	19.99	−1.50	−3.00	1.50
1	19.99	1.50	3.00	1.50
2	12.73	10.00	2.00	2.50
3	12.73	−10.00	−2.00	2.50
4	8.85	−3.60	−0.80	0.80
5	8.85	3.60	0.80	0.80
6	8.42	−3.20	−1.20	0.90
7	8.42	3.20	1.20	0.90

[DOI: 10.22068/ijrare.349]

The evaluation of the identification's resilience to noise is now being conducted. Figure 3 presents examples of noisy signals created at various noise intensities, along with the frequency spectrum for the sample noisy signal that contains the maximum level of noise.

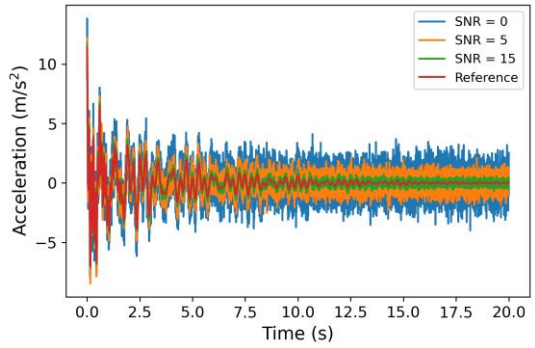

(a)

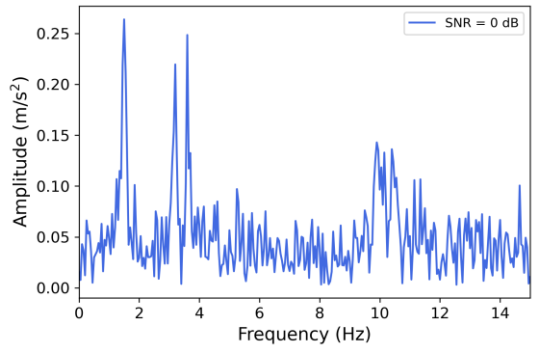

(b)

Figure 3. Synthetic free vibration signals featuring closely spaced modes: (a) noisy synthetic signals across various SNR values, and (b) sample frequency spectrum for the synthetic signal with SNR = 0.

The results presented in Table 2 demonstrate the effectiveness of the MPM in accurately identifying the modal frequencies and damping ratios of a synthetic free vibration signal with closely spaced modes, even in the presence of noise. The analysis was conducted at three different SNRs of 15 dB, 5 dB, and 0 dB to represent varying levels of noise contamination.

Across all tested SNR levels, the identified modal frequencies remain consistent and close to their true values, with small standard deviations. This highlights the robustness of the MPM in frequency identification, even under high noise conditions (SNR = 0 dB). The method's performance is particularly noteworthy for the closely spaced modes (modes 2 and 3), which are successfully identified despite the presence of noise.

In contrast, the identified damping ratios, while remaining close to their true values, exhibit increasing standard deviations as the SNR decreases. This suggests that damping estimation is more sensitive to noise compared to frequency estimation. Nevertheless, the MPM still provides reasonable damping estimates, even at the highest noise level tested (SNR = 0 dB).

The damping ratios showed slight variations: a minimal decrease of approximately −0.33% for Mode 1, −2.5% for Mode 2, an increase of 8.75% for Mode 3, and a significant decrease of −35.64% for Mode 4.

Table 2. Identifying modal frequency and damping ratios in synthetic free vibration with closely spaced modes through noisy data analysis using MPM (mean ± standard deviation)

SNR (dB)	Modal parameters	Mode 1	Mode 2	Mode 3	Mode 4
15	f [Hz]	1.50 ± 0.00	3.20 ± 0.00	3.60 ± 0.00	10.00 ±0.02
	ξ [%]	3.02 ± 0.12	1.20 ± 0.07	0.80 ± 0.04	2.02± 0.60
5	f [Hz]	1.50 ± 0.02	3.20 ± 0.01	3.60 ± 0.03	10.01 ±0.06
	ξ [%]	3.03 ± 0.46	1.20 ± 0.23	0.82 ± 0.27	1.92± 0.77
0	f [Hz]	1.50 ± 0.02	3.20 ± 0.02	3.60 ± 0.02	10.00 ±0.08
	ξ [%]	3.01 ± 0.75	1.17 ± 0.39	0.87 ± 0.43	1.30± 0.92

3.2. Synthetic signal with minor mode

The free response of a system with MDOF, as described by [14], is analyzed through the lens of three overlaid vibration modes, where the total number of modes, N, is set to three. The system exhibits natural frequencies at f_1=1.5 Hz, f_2=3.5 Hz, and f_3=7 Hz, with corresponding modal damping ratios of ξ_1=3%, ξ_2=5%, and ξ_3=3%. The magnitudes of the vibrations for these modes are specified as A_1=1.5, A_2=0.95, A_3=4, with all modes aligned in phase (i.e., φ_n=0 $\forall n$). The analysis incorporates various levels of noise, employing a sampling frequency of F_s=1000 Hz.

[DOI: 10.22068/ijrare.349]

Figure 4 showcases examples of noisy signals generated under different levels of interference, in addition to the frequency spectrum of the sample that is most heavily affected by noise. The frequency spectrum illustrated in Figure 4 reveals that the peak corresponding to the second mode is considerably less pronounced than those related to the first and third modes. Such a condition often emerges when free vibrations are initiated by a force or displacement applied close to the nodal point of a vibration mode that experiences significant damping [4]. As a result, this particular mode receives minimal excitation, which renders its accurate detection a difficult endeavor.

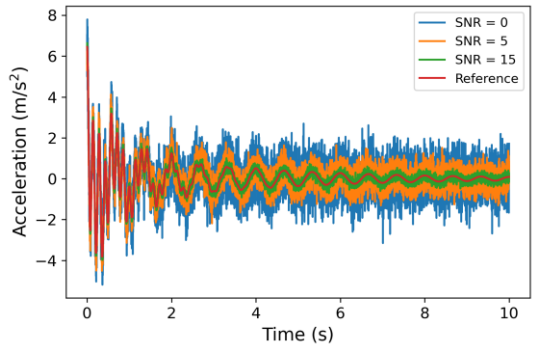

(a)

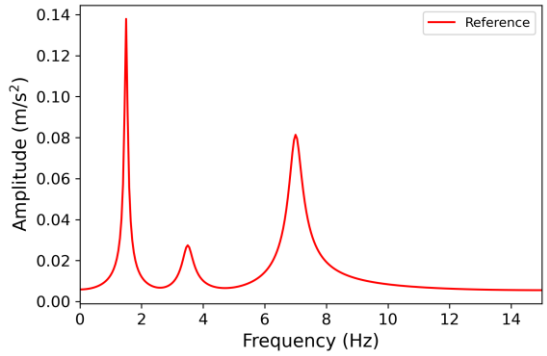

(b)

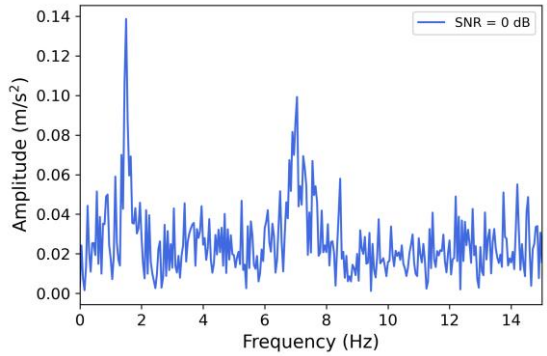

(c)

Figure 4. Synthetic free vibration signals featuring minor mode: (a) noisy synthetic signals across various SNR values, (b) sample frequency spectrum for the noise-free synthetic signal, and (c) sample frequency spectrum for the synthetic signal with SNR = 0.

According to the results presented in Table 3, at an SNR of 15 dB, the frequency estimates exhibit impeccable accuracy across all modes. Conversely, damping ratio estimates demonstrate slight discrepancies, with Mode 2 exhibiting a notable deviation of 15% from its true value, whereas Modes 1 and 3 maintain high fidelity to their actual damping ratios, with discrepancies less than 1%. This variance underscores the sensitivity of damping ratio estimation to noise levels, particularly for Mode 2 (minor mode), which could suggest a heightened susceptibility to noise.

The SNR of 5 dB reveals consistency in frequency estimation. The damping ratio estimations at this SNR level unveil a more pronounced variance, especially for Mode 2, where the estimation deviates by 53.2% from its true value, and to a lesser extent for Mode 3, with a 3.33% deviation.

At the lowest SNR of 0 dB, frequency estimation remains largely unaffected. This consistency in frequency estimation even under significantly reduced SNR levels highlights the MPM's efficacy in frequency identification. This finding aligns with prior research [4]. However, the damping ratio estimations reveal substantial deviations, particularly for Modes 2 and 3, where discrepancies reach 56.8% and 24%, respectively. Such deviations further accentuate the complexity of accurately estimating damping ratios in noise-afflicted environments, emphasizing the importance of advanced signal processing or noise reduction techniques to improve estimation accuracy.

Table 3. Identifying modal frequency and damping ratios in synthetic free vibration with closely spaced modes through noisy data analysis using MPM (mean ± standard deviation)

SNR (dB)	Modal parameters	Mode 1	Mode 2	Mode 3
15	f [Hz]	1.50± 0.00	3.50± 0.06	7.00± 0.02
	ξ [%]	3.00± 0.11	4.25± 1.44	3.03± 0.19
5	f [Hz]	1.50± 0.01	3.51± 0.10	7.00± 0.06
	ξ [%]	3.02± 0.48	2.34± 1.50	2.90± 0.93
0	f [Hz]	1.50± 0.03	3.50± 0.09	7.02± 0.08
	ξ [%]	3.02± 0.75	2.16± 1.55	2.28± 1.16

[DOI: 10.22068/ijrare.349]

4. Experimental application on a truss railway bridge

Since its inauguration for railway use in 1999, the Neka Bridge has showcased an open-deck design with a framework composed of steel trusses. It stretches over a distance of 36 m and has a width of 5.5 m. The bridge's structural integrity is bolstered by four lateral frames constructed from 2IPE180 sections, each standing at a height of 4.8 m, which serve to link the bridge's upper chords. The construction of the top and bottom chords, along with the diagonal braces, utilizes IPBL220 sections. The chords are constructed as built-up elements with four stiffening L-shaped brackets of 80×65×8 mm and two plates of 160×10 mm. At every junction, the chords and diagonal braces are joined through a gusset plate employing bolt connections. Additionally, the bridge comprises 13 floor beams crafted from IPBL400 sections, which are laterally braced at certain intervals using L-shaped brackets of dimensions 120×120×12 mm to maintain stability in the horizontal plane. The bridge's decking is finalized with two stringers made from IPBL240 sections, spaced 1.5 m apart. UIC60 type rails (as per the International Union of Railways standards) traverse this bridge, laid on a non-blasted, open-deck surface. These rails are directly anchored to the bridge's stringers and floor beams with the aid of K-type fasteners (Figure 5) [21,22].

Figure 5. Overview of the Neka truss railway bridge.

The Neka Bridge underwent two distinct forms of load testing: the first involved an impact loading test, where a weight of 35 kg was dropped from a height of 1.65 m, and the second consisted of an EMD GT26 Locomotive crossing the bridge at a velocity of 55 km/h (DNF55). This investigation utilized the free vibration responses from both tests for modal parameter identification. Figure 6 illustrates the placement of accelerometers, their orientation, and the associated time histories. The uniaxial accelerometers have capacities of 2g and 5g, with the frequency range of the 2g accelerometer being 0 to 200 Hz and the frequency range of the 5g accelerometer being 0 to 300 Hz. The sensitivity of the 2g accelerometer is 1 V/g, and the sensitivity of the 5g accelerometer is 400 mV/g. The sampling frequency for recording the acceleration response is set at F_s= 2000 Hz.

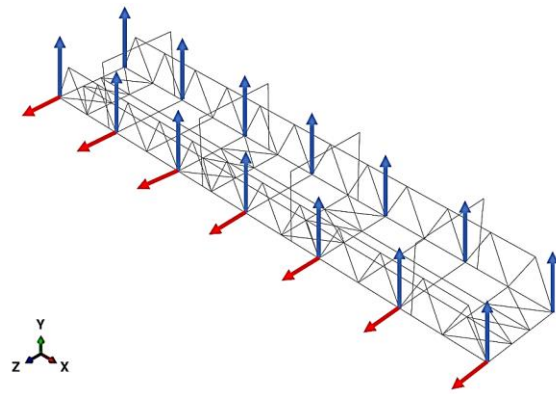

(a)

[DOI: 10.22068/ijrare.349]

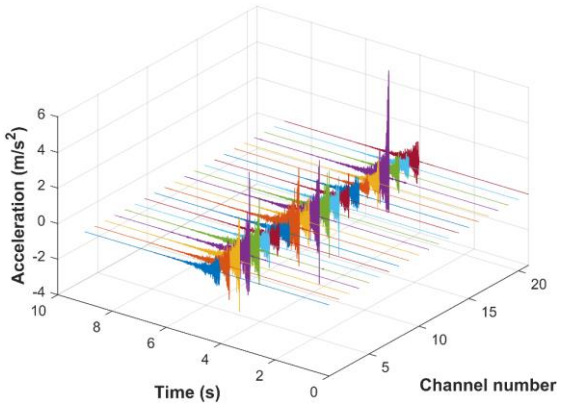

(b)

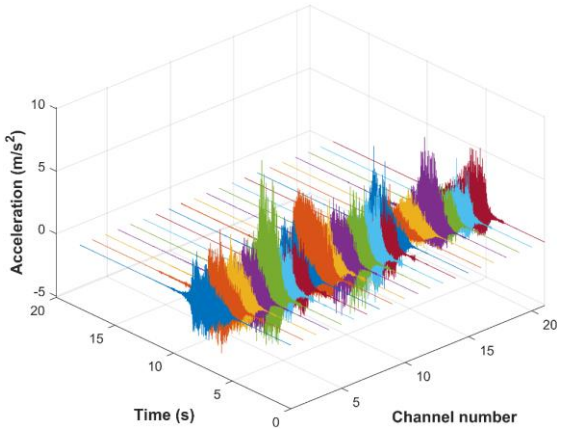

(c)

Figure 6. (a) Accelerometer arrangement and orientation, (b) time histories from impact loading test, and (c) time histories from train passage.

Every recorded signal underwent filtering using a 4th-order Butterworth low-pass filter, aiming to confine the analysis within the desired frequency range (< 25 Hz). Figure 7 illustrates the dynamic response of the railway bridge due to locomotive transit, showcasing both the free vibration response and the corresponding frequency spectrum.

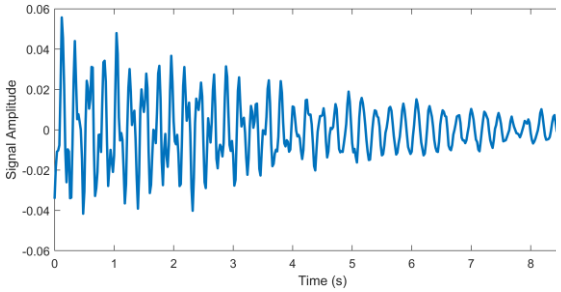

(a)

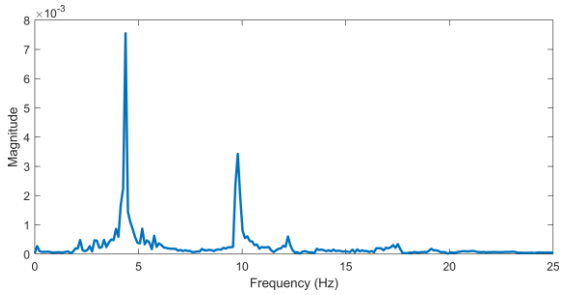

(b)

Figure 7. Dynamic response of the midpoint of the bridge: (a) free vibration acceleration due to locomotive transit, and (b) frequency spectrum of the signal.

Figure 8 showcases a comparative analysis of the averaged frequency spectrum from free vibration responses. It is observed that the impact test exhibits suboptimal efficacy in the identification of low-frequency oscillations when juxtaposed with the locomotive passage test. However, its proficiency in discerning higher-frequency oscillations demonstrates a marked improvement.

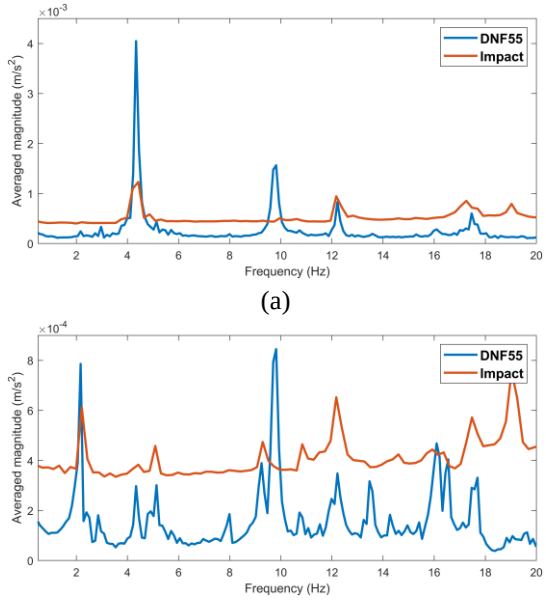

(a)

(b)

Figure 8. Comparative analysis of averaged frequency spectrum for (a) vertical and (b) lateral free vibration responses: impact test vs. locomotive transit (DNF55).

The energy-sorted MPM has been applied to estimate the modal characteristics of the railway bridge. To further validate these findings, the modal properties of the bridge were also assessed using the covariance-based stochastic subspace identification (SSI-COV) [23,24]. Figure 9 illustrates the successful estimation of the free vibration acceleration signal of the

[DOI: 10.22068/ijrare.349]

midpoint accelerometer via the passing locomotive using the energy-sorted MPM. As shown in the figure, the estimated acceleration signal closely follows the measured acceleration signal.

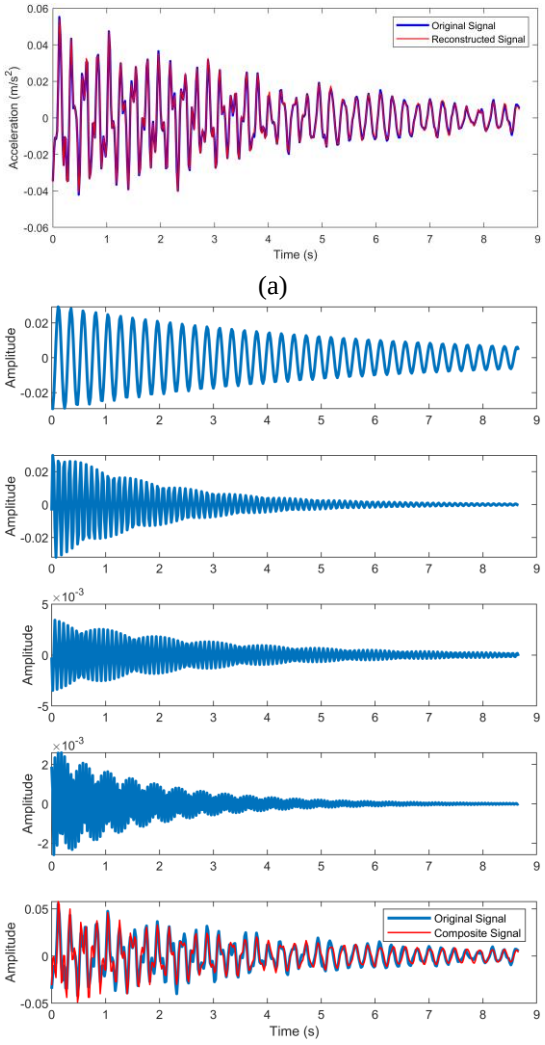

(a)

(b)

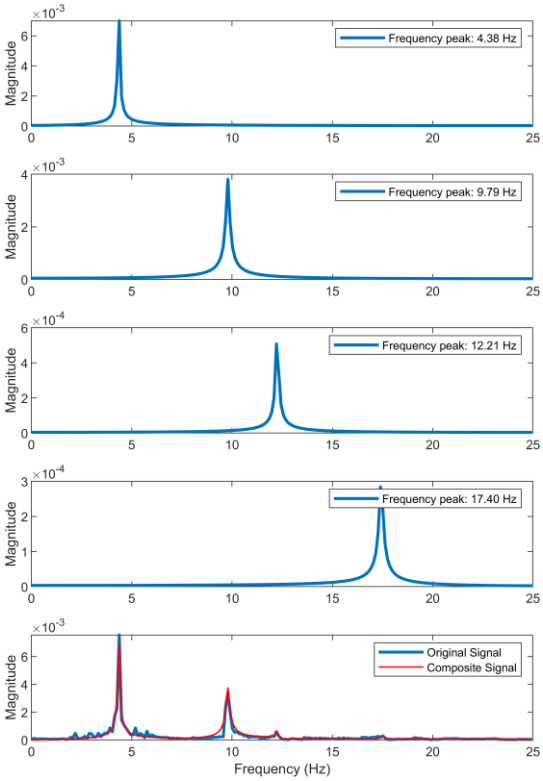

(c)

Figure 9. (a) Free vibration acceleration due to locomotive transit and its reconstructed form via the MPM, (b) the vertical components extracted via MPM, and (c) their corresponding frequency spectrum.

The results in Table 4 show the estimated natural frequencies and damping ratios of the railway bridge obtained using the MPM and the SSI-COV method. The estimates are derived from the free vibration responses of the bridge due to the locomotive transit (DNF55) and the impact loading test (IMPACT).

Table 4. Estimated natural frequencies of the railway bridge using the MPM and SSI-COV methods.

	MPM				SSI-COV			
	DNF55		IMPACT		DNF55		IMPACT	
Mode	f [Hz]	ξ [%]	f [Hz]	ξ [%]	f [Hz]	ξ [%]	f [Hz]	ξ [%]
1	2.20 ± 0.02	2.02 ± 1.35	N/A	N/A	2.17	3.13	2.28	4.22
2	4.36 ± 0.01	0.61 ± 0.09	4.35 ± 0.04	3.23 ± 0.76	4.36	0.84	4.31	2.44
3	5.18 ± 0.05	0.83 ± 0.80	N/A	N/A	5.18	0.91	5.09	1.04
4	9.73 ± 0.07	0.66 ± 0.29	9.41 ± 0.12	0.37 ± 0.07	9.82	0.36	9.28	0.94
5	12.23 ± 0.02	0.44 ± 0.06	12.24 ± 0.01	0.42 ± 0.19	12.24	0.47	12.24	0.62
6	17.59 ± 0.10	0.32 ± 0.24	17.38 ± 0.17	0.99 ± 0.33	17.55	0.91	17.63	0.86
7	N/A	N/A	19.13 ± 0.02	0.62 ± 0.45	N/A	N/A	19.13	0.55
8	N/A	N/A	19.53 ± 0.00	0.54 ± 0.00	N/A	N/A	19.54	0.77

For the locomotive transit case, both MPM and SSI-COV were able to identify the first six modes of the bridge, with natural frequencies ranging from 2.20 Hz to 17.59 Hz for MPM and 2.17 Hz to 17.55 Hz for SSI-COV. The damping ratios estimated by MPM varied from 0.32% to 2.02%, while those estimated by SSI-COV ranged from 0.36% to 3.13%. The results from

[DOI: 10.22068/ijrare.349]

both methods show good agreement, with small differences in the estimated values.

In the case of the impact loading test, MPM identified six modes (2, 4, 5, 6, 7, and 8), with natural frequencies ranging from 4.35 Hz to 19.53 Hz and damping ratios varying from 0.37% to 3.23%. SSI-COV, on the other hand, identified eight modes with natural frequencies ranging from 2.28 Hz to 19.54 Hz and damping ratios varying from 0.55% to 4.22%. The impact loading test results show that both methods were able to identify higher frequency modes (7 and 8) that were not identified in the locomotive transit case.

Furthermore, it is interesting to note the trends in the estimated natural frequencies and damping ratios across the different modes and loading scenarios. For both MPM and SSI-COV, the natural frequencies generally increase with the mode number (Figure 10(a)), which is expected for most structural systems. However, the damping ratios do not exhibit a consistent trend across the modes (Figure 10(b)). In the locomotive transit case, the damping ratios estimated by MPM show a decreasing trend from mode 1 to mode 6, while those estimated by SSI-COV fluctuate without a clear pattern. For the impact loading test, the damping ratios estimated by both methods vary across the modes without a discernible trend.

These observations suggest that the damping characteristics of the railway bridge are more complex and may depend on various factors, such as the mode shape, the interaction between the structure and the surrounding environment, and the nature of the excitation source. Further investigation into the damping mechanisms and their relationship with the modal properties of the bridge could provide valuable insights for understanding its dynamic behavior and for developing more accurate numerical models.

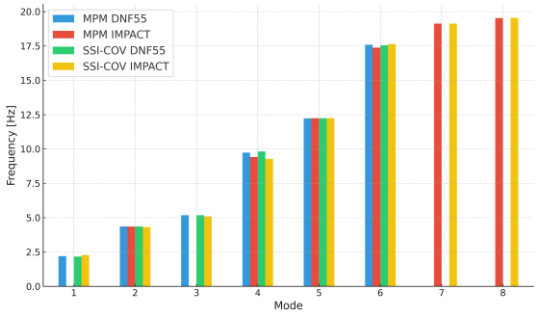

(a)

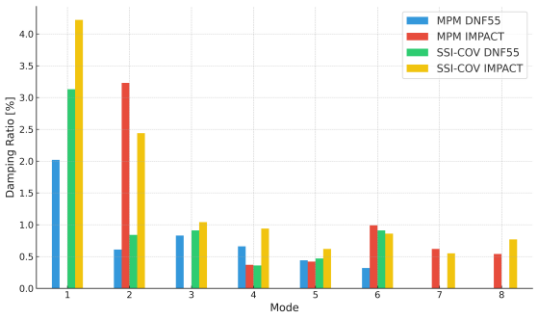

(b)

Figure 10. Estimated modal parameters of the railway bridge employing the MPM and SSI-COV techniques: (a) modal frequencies, and (b) damping ratios.

The vertical mode shapes identified by the MPM approach are presented in Figure 11 using [13].

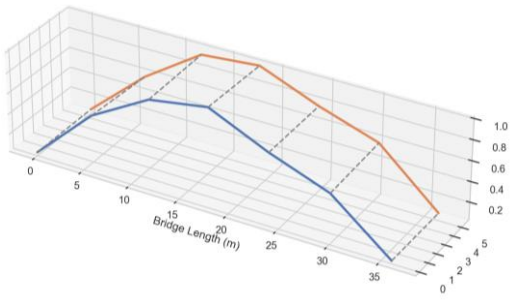

Mode 2

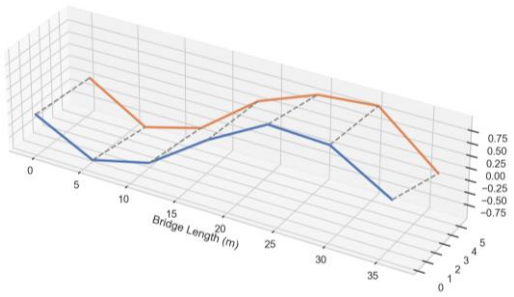

Mode 5

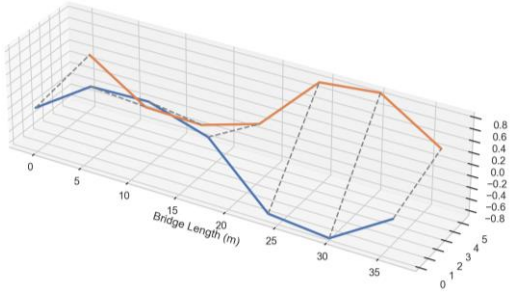

Mode 6

[DOI: 10.22068/ijrare.349]

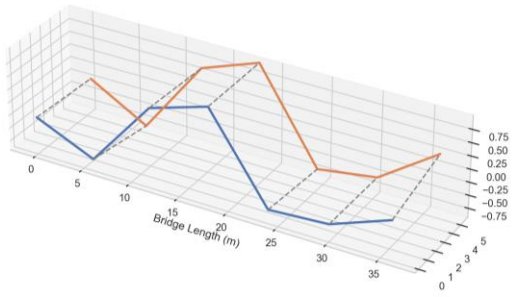

Mode 7

Figure 11. Estimated vertical mode shapes of the railway bridge using the MPM approach.

5. Conclusion

This study successfully demonstrates the applicability and efficiency of the energy-sorted matrix pencil method (MPM) in identifying the modal properties of a truss railway bridge through free vibration response analysis. By meticulously testing the MPM with synthetic signals and applying it to a real-world railway bridge, this research has highlighted the method's capability to accurately determine modal frequencies, damping ratios, and mode shapes.

The numerical validation using synthetic signals revealed the MPM's robustness in extracting modal parameters with high precision, even under varying noise levels. This aspect of the research underscores the method's potential for reliable use in structural health monitoring, especially where environmental noise can be a significant concern.

In its experimental application to the Neka railway bridge, the study provides valuable insights into the dynamic characteristics of the bridge under operational loads. The comparative analysis with the covariance-based stochastic subspace identification (SSI-COV) further establishes the MPM's validity, showcasing good agreement in frequency estimates and reasonable coherence in damping ratios.

The findings from this research carry substantial implications for the field of civil engineering, particularly in the monitoring and maintenance of railway bridge infrastructure. The ability to precisely identify modal parameters is crucial for assessing the structural health and ensuring the safety and longevity of such critical assets.

In conclusion, the energy-sorted MPM, as explored and validated in this study, represents a significant advancement in modal identification techniques. Its successful application in both theoretical and practical frameworks not only validates its effectiveness but also opens up new avenues for future research and development in structural health monitoring.

Declaration of Conflicting Interests

The author(s) declared no potential conflicts of interest with respect to the research, authorship, and/or publication of this article.

References

[1] Gonen S, Demirlioglu K, Erduran E. Modal Identification of a Railway Bridge Under Train Crossings: A Comparative Study. In: Noh HY, Whelan M, Harvey PS, editors. Dynamics of Civil Structures, Volume 2, Cham: Springer International Publishing; 2023, p. 33–40. https://doi.org/10.1007/978-3-031-05449-5_4.

[2] Ataei S, Shariatzadeh M. Displacement monitoring of a Long-Span Arch Railway Bridge using Digital Image Correlation (DIC). International Journal of Railway Research 2021;8:1–12.

[3] Mosleh A, Mohammadi M, Vale C, Ribeiro D, Montenegro P, Meixedo A. Smart detection of wheel defects using artificial intelligence and wayside monitoring system. International Journal of Railway Research 2023;10:9–18.

[4] Mazzeo M, De Domenico D, Quaranta G, Santoro R. An efficient automatic modal identification method based on free vibration response and enhanced Empirical Fourier Decomposition technique. Engineering Structures 2024;298:117046.

[5] Asadi Jafari MH, Zarastvand M, Zhou J. Doubly curved truss core composite shell system for broadband diffuse acoustic insulation. Journal of Vibration and Control 2023:10775463231206229. https://doi.org/10.1177/10775463231206229.

[6] Mazzeo M, De Domenico D, Quaranta G, Santoro R. Automatic modal identification of bridges based on free vibration response and variational mode decomposition

[DOI: 10.22068/ijrare.349]

technique. Engineering Structures 2023;280:115665.
[7] Yang X-M, Yi T-H, Qu C-X, Li H-N, Liu H. Modal identification of high-speed railway bridges through free-vibration detection. Journal of Engineering Mechanics 2020;146:04020107.
[8] Jacobson KE, Kiviaho JF, Kennedy GJ, Smith MJ. Evaluation of time-domain damping identification methods for flutter-constrained optimization. Journal of Fluids and Structures 2019;87:174–88.
[9] Tomaszkiewicz K, Owerko T. Estimation of the bridge damping decrement for in-situ recorded signal with unusual features. Bridge Safety, Maintenance, Management, Life-Cycle, Resilience and Sustainability, CRC Press; 2022, p. 501–8.
[10] Erduran E, Gonen S, Pulatsu B, Soyoz S. Damping in masonry arch railway bridges under service loads: An experimental and numerical investigation. Engineering Structures 2023;294:116801.
[11] Huang F-L, Wang X-M, Chen Z-Q, He X-H, Ni Y-Q. A new approach to identification of structural damping ratios. Journal of Sound and Vibration 2007;303:144–53.
[12] Suvarna S, Shetty N, Date H, Mishra S, Indani T, Kazi F. Energy Sorted Matrix Pencil Method to identify Dominant Modes from Noisy Data. 2020 IEEE 17th India Council International Conference (INDICON), IEEE; 2020, p. 1–7.
[13] Silva A, Ribeiro D, Montenegro PA, Ferreira G, Andersson A, Zangeneh A, et al. New Contributions for Damping Assessment on Filler-Beam Railway Bridges Framed on In2Track EU Projects. Applied Sciences 2023;13:2636.
[14] Rao K, Shubhanga KN. A Comparison of SVD-Augmented Prony Algorithms for Noisy Power System Signals. IEEE Access 2023.
[15] de Prony GR. Essai experimental et analytique: sur les lois de la dilatabilite des fluides elastique et sur celles de la force expansive de la vapeur de l'eau et de la vapeur de l'alkool, a differentes temperatures. Journal Polytechnique Ou Bulletin Du Travail Fait a l'Ecole Centrale Des Travaux Publics 1795.
[16] Hu S-LJ, Yang W-L, Li H-J. Signal decomposition and reconstruction using complex exponential models. Mechanical Systems and Signal Processing 2013;40:421–38.
[17] Fernández Rodríguez A, De Santiago Rodrigo L, López Guillén E, Rodríguez Ascariz JM, Miguel Jiménez JM, Boquete L. Coding Prony's method in MATLAB and applying it to biomedical signal filtering. BMC Bioinformatics 2018;19:451. https://doi.org/10.1186/s12859-018-2473-y.
[18] Sarkar TK, Pereira O. Using the matrix pencil method to estimate the parameters of a sum of complex exponentials. IEEE Antennas and Propagation Magazine 1995;37:48–55.
[19] Trinh W, Shetye K, Idehen I, Overbye T. Iterative matrix pencil method for power system modal analysis 2019.
[20] Bagheri A, Ozbulut OE, Harris DK. Structural system identification based on variational mode decomposition. Journal of Sound and Vibration 2018;417:182–97.
[21] Ataei S, Aghakouchak AA, Marefat MS, Mohammadzadeh S. Sensor fusion of a railway bridge load test using neural networks. Expert Systems with Applications 2005;29:678–83.
[22] Mohammadzadeh S. Load testing of the Neka bridge. Technical report, Railway faculty of engineering, Science and technology University Tehran, Iran; 2004.
[23] Van Overschee P, De Moor B. Subspace identification for linear systems: Theory—Implementation—Applications. Springer Science & Business Media; 2012.
[24] Magalhães F, Caetano E, Cunha Á. Operational modal analysis of the Braga sports stadium suspended roof. Proceedings of the 24th IMAC, St Louis 2006.

[DOI: 10.22068/ijrare.349]